Analytical Methods

Cite this: *Anal. Methods*, 2012, **4**, 1906

www.rsc.org/methods

COMMUNICATION

An Al^{3+} induced green luminescent fluorescent probe for cell imaging and naked eye detection†

Debasis Karak, Sisir Lohar, Animesh Sahana, Subarna Guha, Arnab Banerjee and Debasis Das*

Received 5th March 2012, Accepted 29th April 2012
DOI: 10.1039/c2ay25226k

A novel pyrimidine based Al^{3+} selective fluorescent probe (L) has been synthesised by a facile one step coupling of 4,5-diamino pyrimidine with 2-hydroxy naphthaldehyde. L has been obtained in pure crystalline form without any column chromatographic purification. Upon binding Al^{3+}, the single emission band of L undergoes red shift from 470 nm to dual emission peaks *viz.* 505 nm and 538 nm with appearance of a very intense green luminescence. L could detect as low as 2.9×10^{-7} M Al^{3+} with a binding constant value of 5.4×10^4 M^{-1}. Al^{3+} contaminated cells became green in the presence of L making it suitable for intracellular Al^{3+} detection.

It is well known that aluminum is not an essential element for biological processes. Detection of aluminum is of great interest because of its potential toxicity and widespread application in automobiles, packaging materials, electrical equipment, machinery, food additives, clinical drugs, water purification, building construction, *etc.*[1,2] The leaching of aluminum from soil by acid rain increases free Al^{3+} which is deadly to growing plants.[3] According to a WHO report the average daily human intake of aluminum is approximately 3–10 mg day^{-1}. Tolerable weekly aluminum dietary intake in the human body is estimated to be 7 mg kg^{-1} body weight.[4] The toxicity of aluminum causes damage to the central nervous system, and is suspected to play a role in neurodegenerative diseases like Alzheimer's and Parkinson's diseases. It is also responsible for intoxication in hemodialysis patients.[5] High contents of aluminum in the body can be harmful to the brain and kidneys.[6,7] Aluminum can also damage eco-environmental and biological systems. A very small number of Al^{3+} sensors have been reported,[8] but most of them have involved tedious synthetic protocols and/or the increase of fluorescence intensity is not so high. Naphthalene derivatives have been widely used as an ideal fluorophore for their short fluorescence lifetime,[9] low fluorescence quantum yield[10] and their ability to act as a donor as well as an acceptor.[11] Additionally, fluorescent sensors that work through a ratiometric mechanism[12] can inherently avoid the effect of surrounding conditions like temperature, polarity of media and probe concentration as the ratios of the two emission intensities (at one wavelength the intensity increases while at the other it decreases) are measured as a function of externally added cation concentration.

Our research group is actively engaged in the development of novel Al^{3+} selective fluorescent probes.[8e,f] Herein, we report the facile, inexpensive synthesis and biological application of a novel pyrimidine based ratiometric Al^{3+} selective fluorescent probe (**L**) derived by coupling 4,5-diamino pyrimidine with 2-hydroxy napthaldehyde (Scheme 1). **L** has been obtained in pure crystalline form without any column chromatographic purification. Upon binding Al^{3+}, the single emission band of **L** undergoes red shift from 470 nm to dual emission peaks *viz.* 505 nm and 538 nm with appearance of a very intense green luminescence.

Fig. 1 illustrates the changes of UV-Vis spectra of **L** (100 μM in DMSO) in the presence of Al^{3+}. The absorption spectrum of **L** shows three intense absorption bands at 260, 325 and 380 nm respectively. Upon gradual addition of Al^{3+}, two new broad peaks at 455 nm and 480 nm have appeared, indicating **L**–Al^{3+} complexation. The intensity of the new bands increases with the increase of Al^{3+} concentration. Linear fitting of the titration data at 455 nm is shown in the inset of Fig. 1. **L** has excitation and emission maxima at 365 nm and 470 nm, respectively (ESI, Fig. S1†). Fig. 2 shows the emission spectra of **L** (10 μM) in the presence of different metal ions in DMSO (100 μM). While the addition of various metal ions like Na^+, Mg^{2+}, K^+, Ca^{2+}, Mn^{2+}, Co^{2+}, Ni^{2+}, Cu^{2+}, Zn^{2+}, Ag^+, Cd^{2+}, Hg^{2+} and Pb^{2+} quenches the weak fluorescence of **L**, a strong fluorescence enhancement with a remarkable red shift to the region of 500–600 nm having dual peaks at 505 and 538 nm is observed on addition of Al^{3+} (Fig. 2). Emission intensities of **L** in the presence of other metal ions are shown as the inset of Fig. 2. Additionally, due to the appearance of green luminescence of the solution, it can be easily observed by the naked eye which is the novelty of this probe. The emission intensity of the **L**–Al^{3+} system (at 505 nm and 538 nm) increases gradually on addition of Al^{3+} (4–10 μM) up to 1 : 1 stoichiometry and further addition of

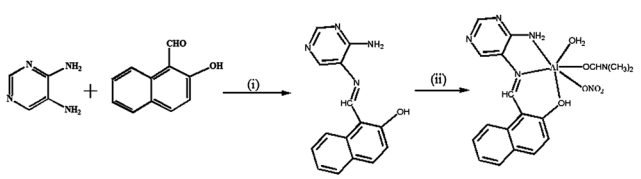

Scheme 1 Synthesis of the receptor **L** and its Al^{3+} complex, (i) MeOH, refluxed for 6 h and (ii) Al $(NO_3)_3 \cdot 9H_2O$ in DMF, refluxed at 80 °C for 2 h.

Department of Chemistry, The University of Burdwan, Burdwan 713104, India. E-mail: ddas100in@yahoo.com; Fax: +91-342-2530452; Tel: +91-342-2533913

† Electronic supplementary information (ESI) available. See DOI: 10.1039/c2ay25226k

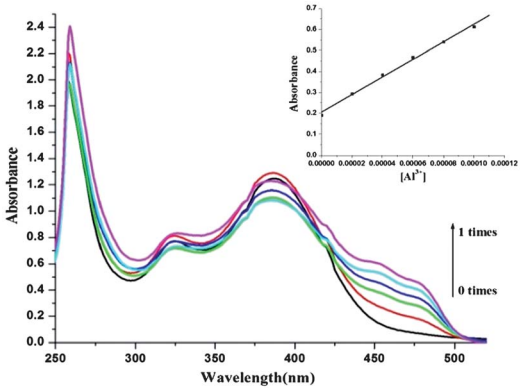

Fig. 1 Changes of the UV-Vis spectra of **L** (100 μM in DMSO) with externally added Al^{3+} (0, 20, 40, 60, 80, and 100 μM). (Inset): absorbance of **L** as a function of [Al^{3+}] at 455 nm.

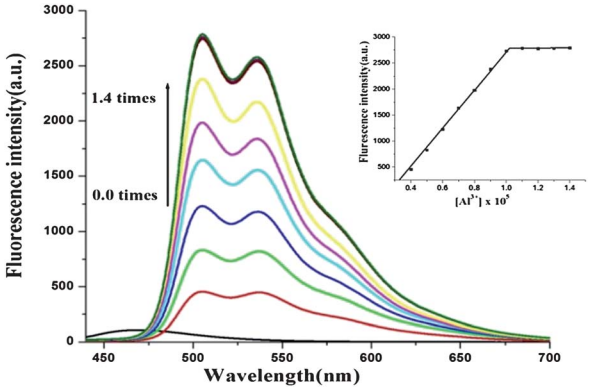

Fig. 3 Emission spectra of **L** (10 μM) in the presence of 0, 4, 5, 6, 7, 8, 9, 10, 11, 12, 13 and 14 μM Al^{3+} in DMSO at room temperature (λ_{ex}, 365 nm). The inset shows the plot of emission intensity *vs.* [Al^{3+}].

Al^{3+} does not change the fluorescence intensity of the system. The maximum fluorescence enhancement (40 fold) has been observed at 505 nm (Fig. 3). The plot of fluorescence intensity *vs.* externally added [Al^{3+}] (inset of Fig. 3) reveals that after a certain amount of externally added Al^{3+} ([Al^{3+}] = 10 μM, [**L**] = 10 μM), there is no further change in the emission intensity of the system. Using this linear relationship (inset of Fig. 3), one can easily determine any unknown Al^{3+} concentration. To calculate the detection limit for Al^{3+} we have used 1 μM of **L** and found the lowest level of detection to be 2.9×10^{-7} (ESI, Fig. S2†). Binding interactions of **L** with Al^{3+} in DMSO solution have been estimated using the Benesi–Hildebrand equation, $(F_\infty - F_0)/(F_x - F_0) = 1 + 1/K_a[C]^n$, where F_0, F_x and F_∞ are the emission intensities of **L** in the absence of Al^{3+}, at an intermediate Al^{3+}, and at a concentration of complete interaction, respectively, where K_a is the binding constant, C is the concentration of Al^{3+} and n is the number of Al^{3+} ions bound per **L** (here, $n = 1$). K_a has the value 5.4×10^4 M^{-1} with $R^2 = 0.989$ (ESI, Fig. S3†). To study the selectivity of **L** towards Al^{3+}, **L** (10 μM) is mixed with 1 equivalent of Al^{3+} in the presence of 5 equivalents of foreign metal ions in a ternary mixture. Fig. S4 (ESI†) shows that the fluorescence intensity of the **L**–Al^{3+} system is quenched upon addition of Cu^{2+}, Fe^{3+} and Cr^{3+}. Job's plot indicates a 1 : 1 (**L** : Al^{3+}, mole ratio) stoichiometry (ESI, Fig. S5†). The response parameter value (α), which is defined as the ratio of the free ligand concentration to the initial concentration of the ligand, is plotted as a function of the Al^{3+} concentration (ESI, Fig. S6†) and can serve as the calibration curve for the determination of unknown [Al^{3+}]. Fluorescence intensity of the [**L**–Al^{3+}] system (20 μM) is highly solvent dependent (ESI, Fig. S7†) and remains unchanged in DMSO solution up to 20 minutes (ESI, Fig. S8†).

Inhibition of internal charge transfer (ICT) and *cis–trans* interconversion due to restricted rotation around the C=N bond of **L** upon binding of Al^{3+} are responsible for the enhancement of fluorescence intensity (Fig. 4).[8b,13] The luminescence of the [**L**–Al^{3+}] system can be detected by the "naked eye" due to the red shift of the emission to the region of 500–600 nm. To the best of our knowledge, this is the first report of an Al^{3+} sensor which shows fluorescence enhancement with red shift, along with green luminescence.

In order to support the binding of Al^{3+} with the receptor **L**, the ^1H NMR titrations have been performed. Different concentrations of Al^{3+} (as its nitrate salt) are added to the DMSO-d_6 solution of **L**. Significant spectral changes have been observed (Fig. 5). The $-NH_2$ peak (H_b) and peaks for *ortho* and *para* hydrogen (H_c and H_d) have been shifted marginally downfield supporting the binding of the $-NH_2$ group with Al^{3+}. The imine C–H peak (H_e) moves towards the downfield region supporting the coordination of the imine nitrogen (–CH=N–) to Al^{3+}. Addition of Al^{3+} to **L** causes loss of the –OH proton first and subsequently the Al^{3+} bonded O atom takes up a proton from the solvent to minimize its positive charge and withdraw electron density from the aromatic ring resulting in the –OH peak (H_a) shifting to up field with the *ortho* proton to the –OH group

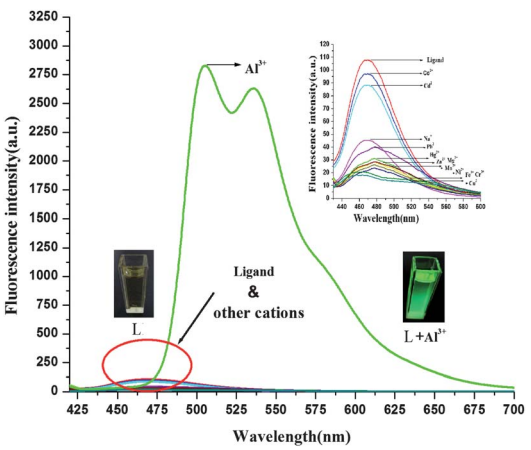

Fig. 2 Emission spectra of **L** (10 μM in DMSO) in the presence of 100 μM of Na^+, Mg^{2+}, Mn^{2+}, Hg^{2+}, Fe^{3+}, Co^{2+}, Ni^{2+}, Cu^{2+}, Cr^{3+}, Zn^{2+}, Cd^{2+}, Pb^{2+} and Al^{3+}, λ_{ex}, 365 nm.

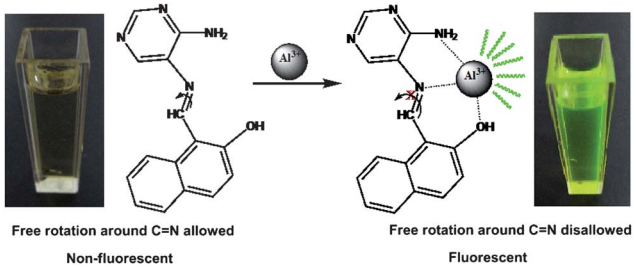

Fig. 4 Proposed binding mode for interaction of Al^{3+} with **L**.

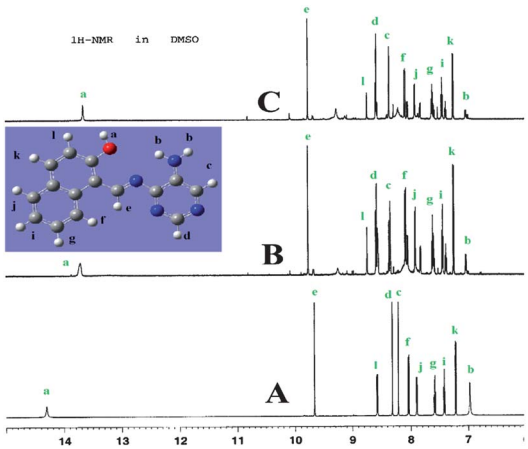

Fig. 5 ^{1}H NMR spectra of **L** with $Al(NO_3)_3 \cdot 9H_2O$ in DMSO-d_6: (A) **L**; (B) **L** with 1 equivalent of Al^{3+} and (C) **L** with 2 equivalents of Al^{3+}.

(H_l) moving towards the downfield region. All other peaks depicted have no significant shifting. Additionally, thermogravimetric studies of free **L** (ESI, Fig. S9†) and the **L**–Al^{3+}complex (ESI, Fig. S10†) provided another support in favor of binding of **L** with Al^{3+}. While **L** has been found to be stable up to 230 °C, the thermal stability of the **L**–Al^{3+} complex is much less (up to 140 °C only).

In order to have the optimized geometry of **L** and its Al^{3+} complex (Fig. 6a) density functional theory (DFT) calculations have been performed using the 6-31G (d) basis set. For **L**–Al^{3+}, LANL2DZ is used. Fig. 6a(A) shows that **L** has a *trans* geometry with respect to the C=N bond. For the **L**–Al^{3+} system, DMF, water and nitrate ion bind to Al^{3+} (also supported from mass spectra). The Highest Occupied Molecular Orbital (HOMO) and the Lowest Unoccupied Molecular Orbital (LUMO) of **L** and its Al^{3+} complex are presented in Fig. 6b which clearly indicates that the **L**–Al^{3+} complex is stabilized by 0.491 eV.

Fig. 7 indicates that **L** can permeate to all types of living cells tested, and causes no harm (as the cells remain alive even after 20 minutes of exposure to **L** at 10 μM). Fig. 7c and d indicate that the cells become green, allowing easy detection of intracellular Al^{3+} in living cells.

In conclusion a highly sensitive fluorescent probe was successfully synthesized for the detection of Al^{3+} in DMSO medium. This probe produces intense green luminescence along with red shift in the presence of Al^{3+}, enabling its naked eye detection. Fluorescence enhancement of **L** in the presence of Al^{3+} is due to the inhibition of ICT and *cis–trans* isomerization around C=N to produce a rigid host–guest framework.

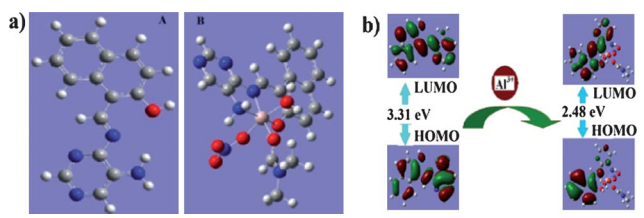

Fig. 6 (a) Energy minimized structures of (A) **L** and (B) **L**–Al^{3+}complex obtained using density functional theoretical calculations. (b) HOMO–LUMO energy gap of **L** and the **L**–Al^{3+}complex.

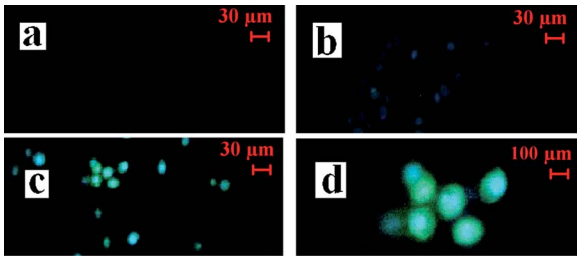

Fig. 7 Fluorescence microscope images of *Candida albicans* cells (IMTECH no. 3018.). *Candida albicans* cells (a); cells treated with **L** (b); Al^{3+} incubated cells treated with **L** (c); and magnified view of (c) (d).

Acknowledgements

The authors sincerely thank West Bengal Council of Science and Technology for financial support. A. Sahana and S. Lohar are thankful to CSIR, New Delhi for providing fellowships. We sincerely thank IICB, Jadavpur and USIC, BU for extending their NMR and fluorescence microscope facilities.

References

1 M. G. Soni, S. M. White, W. G. Flamm and G. A. Burdock, *Regul. Toxicol. Pharmacol.*, 2001, **33**, 66.
2 N. W. Bavlor, W. Egan and P. Richman, *Vaccine*, 2002, **20**, S18.
3 (*a*) E. Delhaize and P. R. Ryan, *Plant Physiol.*, 1995, **107**, 315; (*b*) J. Ren and H. Tian, *Sensors*, 2007, **7**, 3166.
4 (*a*) J. Barcelo and C. Poschenrieder, *Environ. Exp. Bot.*, 2002, **48**, 75; (*b*) B. Valeur and I. Leray, *Coord. Chem. Rev.*, 2000, **205**, 3; (*c*) Z. Krejpcio and R. W. P. Wojciak, *J. Environ. Stud.*, 2002, **11**, 251.
5 (*a*) G. D. Fasman, *Coord. Chem. Rev.*, 1996, **149**, 125; (*b*) P. Nayak, *Environ. Res.*, 2002, **89**, 111; (*c*) C. S. Cronan, W. J. Walker and P. R. Bloom, *Nature*, 1986, **324**, 140; (*d*) G. Berthon, *Coord. Chem. Rev.*, 2002, **228**, 319; (*e*) D. R. Burwen, S. M. Olsen, L. A. Bland, M. J. Arduino, M. H. Reid and W. R. Jarvis, *Kidney Int.*, 1995, **48**, 469.
6 M. Sargazi, N. B. Roberts and A. Shenkin, *J. Inorg. Biochem.*, 2001, **87**, 37.
7 M. I. Yousef, A. M. EI-Morsy and M. S. Hassan, *Toxicology*, 2005, **215**, 97.
8 (*a*) L. Wang, W. Qin, X. Tang, W. Dou, W. Liu, Q. Teng and X. Yao, *Org. Biomol. Chem.*, 2010, **8**, 3751; (*b*) K. K. Upadhyay and A. Kumar, *Org. Biomol. Chem.*, 2010, **8**, 4892; (*c*) D. Maity and T. Govindaraju, *Inorg. Chem.*, 2010, **49**, 7229; (*d*) Y. W. Wang, M. X. Yu, Y. H. Yu, Z. P. Bai, Z. Shen, F. Y. Li and X. Z. You, *Tetrahedron Lett.*, 2009, **50**, 6169; (*e*) A. Sahana, A. Banerjee, S. Das, S. Lohar, D. Karak, B. Sarkar, S. K. Mukhopadhyay, A. K. Mukherjee and D. Das, *Org. Biomol. Chem.*, 2011, **9**, 5523; (*f*) A. Banerjee, A. Sahana, S. Das, S. Lohar, S. Guha, B. Sarkar, S. K. Mukhopadhyay, A. K. Mukherjee and D. Das, *Analyst*, 2012, **137**, 2166; (*g*) D. Maity and T. Govindaraju, *Chem. Commun.*, 2010, **46**, 4499.
9 D. P. Roek, J. E. Chateauneuf and J. F. Brennecke, *Ind. Eng. Chem. Res.*, 2000, **39**, 3090.
10 P. Frederick, F. P. Schwarz and S. P. Wasik, *Anal. Chem.*, 1976, **48**, 524.
11 M. Ali, M. Jha, S. K. Das and S. K. Saha, *J. Phys. Chem. B*, 2009, **113**, 15563.
12 (*a*) A. H. H. Wang, L. Xue, Y. Y. Qian and H. Jiang, *Org. Lett.*, 2010, **12**, 292; (*b*) C. Lu, Z. Xu, J. Cui, R. Zhang and X. Qian, *J. Org. Chem.*, 2007, **72**, 3554; (*c*) J. Wang, H. Liu, W. Wang, I. Kim and C. Ha, *Dalton Trans.*, 2009, 10422; (*d*) S. Goswami, D. Sen and N. K. Das, *Org. Lett.*, 2010, **12**, 856.
13 J.-S. Wu, W.-M. Liu, X.-Q. Zhuang, F. Wang, P.-F. Wang, S.-L. Tao, X.-H. Zhang, S.-K. Wu and S.-T. Lee, *Org. Lett.*, 2007, **9**, 33.

